Comparing the Properties of Homologous Phosphido and Amido Complexes: Synthesis and Characterization of the Disilylphosphido Complexes $\{M[P(SiMe_3)_2]_2\}_2$ Where M = Zn, Cd, Hg, Sn, Pb, and Mn

Subhash C. Goel, Michael Y. Chiang, David J. Rauscher, and William E. Buhro*

Contribution from the Department of Chemistry, Washington University, St. Louis, Missouri 63130. *Received July 7, 1992. Revised Manuscript Received September 23, 1992*

Abstract: Complexes of empirical formula $M[P(SiMe_3)_2]_2$ are prepared in 68–90% yields from $M[N(SiMe_3)_2]_2$ and $HP(SiMe_3)_2$ (M = Zn (**1**), Cd (**2**), Hg (**3**), Sn (**4**), Pb (**5**), Mn (**6**)). All of **1**–**6** are crystalline, air-sensitive, hydrocarbon-soluble solids. Compounds **1** and **2** sublime at 140 °C and 10^{-4} Torr. Compound **6** crystallizes as a THF adduct (**6**·THF); the THF ligand is easily removed in vacuo. X-ray crystallography reveals that **1**–**3** and **5** are solid-state dimers having the structure $\{M[P(SiMe_3)_2][\mu\text{-}P(SiMe_3)_2]\}_2$ and that **6**·THF has the structure $[(Me_3Si)_2P]Mn[\mu\text{-}P(SiMe_3)_2]_2Mn[P(SiMe_3)_2](THF)$. The phosphido bridges are symmetric in **1**, **2**, **5**, and **6** and asymmetric in **3**; the longer bridge distance in **3** (3.246 (1) Å) is a secondary bond. The compounds are also dimeric in solution except for **3**, which is monomeric. Compounds **1** and **2** undergo bridging-to-terminal site exchange. The barriers calculated from the $^{31}P\{^1H\}$ NMR coalescence points are ΔG^*_{360} = 14.3 (2) kcal/mol and ΔG^*_{321} = 12.7 (6) kcal/mol for **1** and **2**, respectively. The barriers calculated from the ^1H NMR coalescence points are ΔG^*_{281} = 14.8 (1) kcal/mol and ΔG^*_{246} = 12.4 (1) kcal/mol for **1** and **2**, respectively. Compounds **4** and **5** exhibit trans ⇄ cis equilibria in solution; **5** crystallizes as the cis isomer. The thermodynamic quantities for the trans ⇄ cis equilibria derived from NMR measurements are ΔH = −1.8 (1) kcal/mol and ΔS = −4.7 (2) eu for **4** and ΔH = −1.4 (1) kcal/mol and ΔS = −4.4 (2) eu for **5**. In general, the $P(SiMe_3)_2$ complexes exhibit higher molecularities and higher coordination numbers than the homologous $N(SiMe_3)_2$ complexes, which indicates that $P(SiMe_3)_2$ ligands have stronger bridging tendencies than do $N(SiMe_3)_2$ ligands. The differing behaviors of the two ligands are ascribed to periodic trends that distinguish the properties of N and P. Crystal data for **1**: triclinic, $P\bar{1}$, a = 9.831 (2) Å, b = 10.813 (2) Å, c = 12.692 (3) Å, α = 80.97 (3)°, β = 67.62 (3)°, γ = 80.20 (3)°, V = 1223.1 (4) Å^3, T = 22 °C, Z = 1. Crystal data for **2**: triclinic, $P\bar{1}$, a = 9.749 (3) Å, b = 10.879 (3) Å, c = 13.078 (4) Å, α = 92.29 (2)°, β = 112.93 (2)°, γ = 98.19 (2)°, V = 1257.4 (6) Å^3, T = 22 °C, Z = 1. Crystal data for **3**: triclinic, $P\bar{1}$, a = 9.817 (2) Å, b = 12.216 (2) Å, c = 12.968 (3) Å, α = 61.94 (1)°, β = 67.99 (1)°, γ = 68.53 (2)°, V = 1237.6 (4) Å^3, T = 22 °C, Z = 1. Crystal data for **5**: orthorhombic, $P2_12_12_1$, a = 13.154 (7) Å, b = 18.343 (13) Å, c = 20.622 (7) Å, V = 4976 (5) Å^3, T = 22 °C, Z = 4. Crystal data for **6**·THF: triclinic, $P\bar{1}$, a = 10.107 (3) Å, b = 16.581 (4) Å, c = 17.234 (4) Å, α = 85.74 (2)°, β = 82.46 (2)°, γ = 72.12 (2)°, V = 2723.2 (12) Å^3, T = 22 °C, Z = 2.

Herein we describe the first members of a new class of inorganic compounds: homoleptic disilylphosphido complexes of empirical formula $M[P(SiMe_3)_2]_x$ ($x \neq 1$). The $P(SiMe_3)_2$ ligand is a heavier congener to the well-known $N(SiMe_3)_2$ ligand, which was significant to the development of low-coordinate metal complexes.[1] The bulky $N(SiMe_3)_2$ stabilizes 2- and 3-coordinate metal-atom environments; this property has allowed a wide range of stable, volatile, low-molecularity, disilylamido derivatives $M[N(SiMe_3)_2]_x$ to be prepared.[2] Homoleptic disilylamido complexes make up the largest known class of amidometal complexes,[2] and because of their general availability, they are commonly used starting materials.[3] New disilylamido complexes of main-group,[4] transition,[5] and f-block elements[6] continue to be reported.

This report provides the first opportunity to compare homologous binary amido and phosphido complexes. We describe the preparation of six homoleptic $P(SiMe_3)_2$ complexes and the X-ray crystal structures of five of them, which reveal the geometrical and coordination tendencies of the $P(SiMe_3)_2$ ligand. The structural, stereochemical, and dynamic properties of the new disilylphosphido compounds have also been examined in solution by variable-temperature NMR spectroscopy. In comparisons of analogous $N(SiMe_3)_2$ and $P(SiMe_3)_2$ complexes, the phosphido compounds exhibit higher molecularities, higher coordination numbers, and configurational effects that are absent in the amido compounds. Our results demonstrate the stronger bridging tendencies of phosphido ligands relative to amido ligands. The differing behaviors of disilylamido and disilylphosphido ligands may be ascribed to normal periodic trends, which distinguish the properties of the second- and third-period elements N and P.

Although efforts to prepare homoleptic phosphido (PR_2) complexes were initiated by Issleib and co-workers 30 years ago,[7] significant progress came much later through the work of Baker,[8] Cowley,[9] Jones,[9,10] du Mont,[11] and Schumann[12] with bulky di-

(1) (a) Bürger, H.; Sawodny, W.; Wannagat, U. *J. Organomet. Chem.* **1965**, *3*, 113. (b) Bürger, H.; Wannagat, U. *Monatsh. Chem.* **1964**, *95*, 1099. (c) Bürger, H.; Wannagat, U. *Monatsh. Chem.* **1963**, *94*, 1007.

(2) Lappert, M. F.; Power, P. P.; Sanger, A. R.; Srivastava, R. C. *Metal and Metalloid Amides*; Ellis Horwood: Chichester, England, 1980.

(3) Caulton, K. G.; Hubert-Pfaltzgraf, L. G. *Chem. Rev.* **1990**, *90*, 969.

(4) (a) Chen, H.; Olmstead, M. M.; Shoner, S. C.; Power, P. P. *J. Chem. Soc., Dalton Trans.* **1992**, 451. (b) Power, P. P.; Ruhlandt-Senge, K.; Shoner, S. C. *Inorg. Chem.* **1991**, *30*, 5013. (c) Björgvinsson, M.; Heinze, T.; Roesky, H. W.; Pauer, F.; Stalke, D.; Sheldrick, G. M. *Angew. Chem., Int. Ed. Engl.* **1991**, *30*, 1677. (d) Westerhausen, M. *Inorg. Chem.* **1991**, *30*, 96. (e) Vaartstra, B. A.; Huffman, J. C.; Streib, W. E.; Caulton, K. C. *Inorg. Chem.* **1991**, *30*, 121. (f) Björgvinsson, M.; Roesky, H. W.; Pauer, F.; Stalke, D.; Sheldrick, G. M. *Inorg. Chem.* **1990**, *29*, 5140. (g) Tesh, K. F.; Hanusa, T. P.; Huffman, J. C. *Inorg. Chem.* **1990**, *29*, 1584. (h) Hitchcock, P. B.; Lappert, M. F.; Lawless, G. A.; Royo, B. *J. Chem. Soc., Chem. Commun.* **1990**, 1141. (i) Clegg, W.; Compton, N. A.; Errington, R. J.; Norman, N. C.; Wishart, N. *Polyhedron* **1989**, *8*, 1579.

(5) (a) Olmstead, M. M.; Power, P. P.; Shoner, S. C. *Inorg. Chem.* **1991**, *30*, 2547. (b) Ellison, J. J.; Power, P. P.; Shoner, S. C. *J. Am. Chem. Soc.* **1989**, *111*, 8044. (c) Chen, H.; Bartlett, R. A.; Dias, H. V. R.; Olmstead, M. M.; Power, P. P. *J. Am. Chem. Soc.* **1989**, *111*, 4338. (d) Andersen, R. A.; Faegri, K., Jr.; Green, J. C.; Haaland, A.; Lappert, M. F.; Leung, W.-P.; Rypdal, K. *Inorg. Chem.* **1988**, *27*, 1782.

(6) (a) Evans, W. J.; Drummond, D. K.; Zhang, H.; Atwood, J. L. *Inorg. Chem.* **1988**, *27*, 575. (b) Boncella, J. M.; Andersen, R. A. *Organometallics* **1985**, *4*, 205. (c) Tilley, T. D.; Andersen, R. A.; Zalkin, A. *Inorg. Chem.* **1984**, *23*, 2271.

(7) The first homoleptic phosphido complexes prepared by Issleib and co-workers in the 1960s are not fully characterized by modern standards, and uncertainty regarding their structures and identities remains. (a) Issleib, K.; Wenschuh, E. *Chem. Ber.* **1964**, *97*, 715. (b) Issleib, K.; Wenschuh, E. *Z. Naturforsch., B: Anorg. Chem., Org. Chem., Biochem., Biophys., Biol.* **1964**, *19B*, 199. (c) Issleib, K.; Fröhlich, H.-O.; Wenschuh, E. *Chem. Ber.* **1962**, *95*, 2742. (d) Issleib, K.; Fröhlich, H.-O. *Chem. Ber.* **1962**, *95*, 375.

(8) Baker, R. T.; Krusic, P. H.; Tulip, T. H.; Calabrese, J. C.; Wreford, S. S. *J. Am. Chem. Soc.* **1983**, *105*, 6763.

0002-7863/93/1515-160$04.00/0

Table I. Spectroscopic Data for Disilylphosphido Complexes

compound	IR (cm^{-1}, KBr)	^1H NMR (δ)[a]	$^{31}P\{^1H\}$ NMR (ppm)[a]
$\{Zn[P(SiMe_3)_2]_2\}_2$ (**1**)	2950 s, 2989 m, 1400 w, 1249 vs, 1242 vs, 978 s, 827 vs, 751 m, 685 m, 628 vs, 464 m, 455 w, 427 m, 414 m	0.50 (br s, 72 H)[b]	−183.0 (br s, bridging); −237.3 (br s, terminal)[b,c]
$\{Cd[P(SiMe_3)_2]_2\}_2$ (**2**)	2949 m, 2893 w, 1399 w, 1385 w, 1242 s, 1060 w, 831 vs, 750 w, 686 m, 627 m, 465 w, 416 w	0.48 (br s, 72 H)[b]	−180.1 (v br s, bridging); −229.5 (v br s, terminal)[b,c]
$\{Hg[P(SiMe_3)_2]_2\}_2$ (**3**)	2951 m, 2892 w, 1385 w, 1244 s, 1059 w, 831 vs, 750 w, 688 w, 627 m, 464 w, 412 w	0.36 (d, $^3J_{H-P}$ = 4.5 Hz, 36 H)[d]	−162.0 (s)[d]
$\{Sn[P(SiMe_3)_2]_2\}_2$ (**4**)	2948 w, 2891 w, 1400 w, 1244 m, 1000 w, 834 vs, 747 w, 682 w, 626 m, 458 vw, 441 vw	0.71 (d, $^3J_{H-P}$ = 4.9 Hz, 0.67 × 18 H, cis bridging); 0.59 (d, $^3J_{H-P}$ = 4.4 Hz, 0.33 × 36 H, trans bridging); 0.51 (d, $^3J_{H-P}$ = 3.4 Hz, 0.67 × 18 H, cis bridging); 0.47 (d, $^3J_{H-P}$ = 4.4 Hz, 0.33 × 36 H, trans terminal);[e] 0.46 (d, $^3J_{H-P}$ = 3.7 Hz, 0.67 × 36 H, cis terminal)[e,f]	−231.8 (s, $^1J_{P-Sn}$ = 1117 Hz, 16%, trans terminal); −236.4 (s, $^1J_{P-Sn}$ = 1012 Hz, 16%, cis terminal); −268.0 (s, $^1J_{P-Sn}$ = 1224 Hz, 27%, cis bridging); −295.3 (s, $^1J_{P-Sn}$ = 1298 Hz, 26%, trans bridging)[f-h]
$\{Pb[P(SiMe_3)_2]_2\}_2$ (**5**)	2944 m, 2893 m, 1397 w, 1259 m, 1243 s, 1066 vw, 832 vs, 745 w, 680 w, 624 s, 460 w, 442 w, 407 s	0.76–0.70 (m, 0.56 × 18 H, cis bridging); 0.57–0.51 (m, 0.44 × 36 H, trans bridging); 0.44–0.38 (m, 0.44 × 18 H, cis bridging);[i] 0.41 (d, $^3J_{H-P}$ = 4.4 Hz, 0.44 × 36 H, trans terminal);[e] 0.40 (d, $^3J_{H-P}$ = 4.4 Hz, 0.56 × 36 H, cis terminal)[e,j]	−217.3 (s, $^1J_{P-Pb}$ = 1264 Hz, 20%, trans terminal); −218.0 (s, $^1J_{P-Pb}$ = 1183 Hz, 20%, cis terminal); −281.4 (s, $^1J_{P-Pb}$ = 1598 Hz, 32%, cis bridging); −302.4 (s, $^1J_{P-Pb}$ = 1658 Hz, 32%, trans bridging)[f,h]
$\{Mn[P(SiMe_3)_2]_2\}_2$·(THF) (**6**·THF)	2953 m, 2895 w, 1248 s, 1060 w, 907 w, 837 vs, 750 w, 688 w, 626 m, 466 w		

[a] NMR spectra were recorded at room temperature in benzene-d_6 except where noted: 300 MHz for ^1H and 121 MHz for ^{31}P. [b] The compound is fluxional; see text. [c] Terminal- and bridging-ligand assignments are explained in the text. [d] Although **3** is dimeric in the solid state; it is apparently monomeric in solution; see text. [e] Overlapping resonance. [f] Cis- and trans-isomer assignments are explained in the text. [g] $^{31}P-^{117}Sn$ and $^{31}P-^{119}Sn$ couplings were not resolved. [h] Percentages given are the satellite intensities. [i] Obscured resonance. [j] In toluene-d_8.

alkylphosphido ligands.[13] However, homoleptic $P(SiMe_3)_2$ complexes, which might be expected to share the stabilities and other properties of $N(SiMe_3)_2$ compounds, had not been described.[14] We initially became interested in $P(SiMe_3)_2$ complexes for their potential as precursors in solution-phase molecular routes to inorganic phosphides.[17] In a communication, we reported that $\{Cd[P(SiMe_3)_2]_2\}_2$ gave Cd_3P_2 by alcoholysis and polycondensation according to eq 1.[17] Consequently, we sought to prepare a series

$$\tfrac{1}{2}\{Cd[P(SiMe_3)_2]_2\}_2 + 4MeOH \xrightarrow{-4MeOSiMe_3} \tfrac{1}{3}Cd_3P_2 + \tfrac{4}{3}PH_3 \quad (1)$$

of $M[P(SiMe_3)_2]_x$ compounds, in part to examine the scope of eq 1 chemistry. We have now obtained new $M[P(SiMe_3)_2]_x$ derivatives of monovalent (M = Li, Na, K, Cu(I)), divalent (M = Mg, Zn, Cd, Hg, Sn(II), Pb(II), Mn(II)), and trivalent (M = In, Bi(III)) metals, and in this first full report, we focus on the complexes of divalent metals having dinuclear structures.

Results

Synthesis and Properties. The new compounds **1–6** were prepared in 68–90% yields by the substitution reaction of eq 2. All

$$M[N(SiMe_3)_2]_2L + 2HP(SiMe_3)_2 \longrightarrow \tfrac{1}{2}\{M[P(SiMe_3)_2]_2\}_2L + 2HN(SiMe_3)_2 \quad (2)$$

M = Zn (**1**)	L = none
Cd (**2**)	none
Hg (**3**)	none
Sn (**4**)	none
Pb (**5**)	none
Mn (**6**·THF)	THF

were isolated as crystalline solids and were characterized by elemental analyses (C, H, N, M except Sn) and IR, ^1H, and ^{31}P NMR spectroscopy (see Table I). The manganese compound **6** crystallized as a THF adduct (**6**·THF), but the THF ligand was easily lost in vacuo, leaving unsolvated $\{Mn[P(SiMe_3)_2]_2\}_2$ (**6**) as a sticky solid. All of **1–6** were soluble in hydrocarbon solvents with gentle warming, and all inflamed spontaneously in air. Only **1** and **2** were sufficiently stable and volatile to sublime at 10^{-4} Torr, with recoveries of 53 and 75%, respectively (see the Experimental Section).

The new compounds exhibited varying degrees of thermal stability. Complexes **1** and **2** decomposed gradually over several days in refluxing toluene according to eq 3. The $[MP(SiMe_3)]_n$

$$\tfrac{1}{2}\{M[P(SiMe_3)_2]_2\}_2 \xrightarrow{\Delta} (1/x)[MP(SiMe_3)]_x + P(SiMe_3)_3 \quad (3)$$

M = Zn, Cd

(9) (a) Benac, B. L.; Cowley, A. H.; Jones, R. A.; Nunn, C. M.; Wright, T. C. *J. Am. Chem. Soc.* **1989**, *111*, 4986. (b) Carrano, C. J.; Cowley, A. H.; Giolando, D. M.; Jones, R. A.; Nunn, C. M.; Power, J. M. *Inorg. Chem.* **1988**, *27*, 2709. (c) Cowley, A. H.; Giolando, D. M.; Jones, R. A.; Nunn, C. M.; Power, J. M. *Polyhedron* **1988**, *7*, 1909. (d) Arif, A. M.; Benac, B. L.; Cowley, A. H.; Jones, R. A.; Kidd, K. B.; Nunn, C. M. *New J. Chem.* **1988**, *12*, 553. (e) Cowley, A. H.; Giolando, D. M.; Jones, R. A.; Nunn, C. M.; Power, J. M. *J. Chem. Soc., Chem. Commun.* **1988**, 208. (f) Arif, A. M.; Benac, B. L.; Cowley, A. H.; Geerts, R.; Jones, R. A.; Kidd, K. B.; Power, J. M.; Schwab, S. T. *J. Chem. Soc., Chem. Commun.* **1986**, 1543. (g) Arif, A. M.; Cowley, A. H.; Jones, R. A.; Power, J. M. *J. Chem. Soc., Chem. Commun.* **1986**, 1446.

(10) Jones, R. A.; Lasch, J. G.; Norman, N. C.; Whittlesey, B. R.; Wright, T. C. *J. Am. Chem. Soc.* **1983**, *105*, 6184.

(11) (a) du Mont, W.-W.; Grenz, M. *Chem. Ber.* **1985**, *118*, 1045. (b) du Mont, W.-W. *Angew. Chem., Int. Ed. Engl.* **1980**, *19*, 554. (c) du Mont, W.-W.; Kroth, H.-J. *Angew. Chem., Int. Ed. Engl.* **1977**, *16*, 792.

(12) Schumann, H.; Frisch, G.-M. *Z. Naturforsch., B: Anorg. Chem., Org. Chem.* **1979**, *34B*, 748.

(13) See also: (a) Hey-Hawkins, E.; Sattler, E. *J. Chem. Soc., Chem. Commun.* **1992**, 775. (b) Alcock, N. W.; Degnan, I. A.; Wallbridge, M. G. H.; Powell, H. R.; McPartlin, M.; Sheldrick, G. M. *J. Organomet. Chem.* **1989**, *361*, C33. (c) Hey, E.; Engelhardt, L. M.; Raston, C. L.; White, A. H. *Angew. Chem., Int. Ed. Engl.* **1987**, *26*, 81. (d) Eichbichler, J.; Peringer, P. *Transition Met. Chem. (London)* **1981**, *6*, 313. (e) Baudler, M.; Zarkadas, A. *Chem. Ber.* **1972**, *105*, 3844.

(14) Heteroleptic complexes of the $P(SiMe_3)_2$ ligand have been studied extensively by Schäfer[15] and Weber.[16]

(15) (a) Schäfer, H.; Leske, W. *Z. Anorg. Allg. Chem.* **1987**, *550*, 57. (b) Schäfer, H.; Binder, D.; Deppisch, B.; Mattern, G. *Z. Anorg. Allg. Chem.* **1987**, *546*, 79. (c) Schäfer, H.; Binder, D. *Z. Anorg. Allg. Chem.* **1987**, *546*, 55. (d) Deppisch, B.; Schäfer, H. *Z. Anorg. Allg. Chem.* **1982**, *490*, 129. (e) Schäfer, H. *Z. Anorg. Allg. Chem.* **1979**, *459*, 157.

(16) (a) Weber, L.; Schumann, H.; Boese, R. *Chem. Ber.* **1990**, *123*, 1779. (b) Weber, L. *Phosphorus Sulfur Relat. Elem.* **1987**, *30*, 311. (c) Weber, L.; Meine, B.; Boese, R.; Augart, N. *Organometallics* **1987**, *6*, 2484. (d) Weber, L.; Bungardt, D. *J. Organomet. Chem.* **1986**, *311*, 269. (e) Weber, L.; Reizig, K.; Frebel, M. *Chem. Ber.* **1986**, *119*, 1857.

(17) (a) Goel, S. C.; Chiang, M. Y.; Buhro, W. E. *J. Am. Chem. Soc.* **1990**, *112*, 5636. (b) See also: Matchett, M. A.; Viano, A. M.; Adolphi, N. L.; Stoddard, R. D.; Buhro, W. E.; Conradi, M. S.; Gibbons, P. C. *Chem. Mater.* **1992**, *4*, 508.

Table II. Crystallographic Data for **1**–**3**, **5**, and **6**·THF

	1	**2**	**3**	**5**	**6**·THF
chemical formula	$C_{24}H_{72}Si_8P_4Zn_2$	$C_{24}H_{72}Si_8P_4Cd_2$	$C_{24}H_{72}Si_8P_4Hg_2$	$C_{24}H_{72}Si_8P_4Pb_2$	$C_{28}H_{80}OSi_8P_4Mn_2$
a (Å)	9.831 (2)	9.749 (3)	9.817 (2)	13.154 (7)	10.107 (3)
b (Å)	10.813 (2)	10.879 (3)	12.216 (2)	18.343 (13)	16.581 (4)
c (Å)	12.692 (3)	13.078 (4)	12.968 (3)	20.622 (7)	17.234 (4)
α (deg)	80.97 (3)	92.29 (2)	61.94 (1)	90.0	85.74 (2)
β (deg)	67.62 (3)	112.93 (2)	67.99 (1)	90.0	82.46 (2)
γ (deg)	80.20 (3)	98.19 (2)	68.53 (2)	90.0	72.12 (2)
V (Å^3)	1223.1 (4)	1257.4 (6)	1237.6 (4)	4976 (5)	2723.2 (12)
Z	1	1	1	4	2
formula weight	840.2	934.2	1110.6	1123.8	891.4
space group	$P\bar{1}$	$P\bar{1}$	$P\bar{1}$	$P2_12_12_1$	$P\bar{1}$
T (°C)	22	22	22	22	22
λ (Å)	1.541 78	0.710 73	0.710 73	0.710 73	0.710 73
ρ_{calcd} (g/cm^3)	1.141	1.234	1.490	1.500	1.087
μ (cm^{-1})	45.18	11.70	65.27	71.40	7.53
$R(F_o)^a$	0.0741	0.0303	0.0337	0.0528	0.0474
$R_w(F_o)^b$	0.1102[c]	0.0354[d]	0.0397[e]	0.0444[f]	0.0533[d]

[a] $R(F_o) = \sum||F_o| - |F_c||/\sum|F_o|$. [b] $R_w(F_o) = (\sum w||F_o| - |F_c||^2/\sum w|F_o|^2)^{1/2}$, $w = [\sigma^2(F_o) + g(F_o)^2]^{-1}$. [c] $g = 0.0211$. [d] $g = 0.0004$. [e] $g = 0.0006$. [f] $g = 0.0001$.

products (M = Zn or Cd) so obtained were insoluble and were characterized by elemental analyses and IR spectroscopy. The latter indicated that the $SiMe_3$ groups remained intact. The structures of these decomposition products $[MP(SiMe_3)]_n$ are unknown. Compounds **3** and **4** decomposed in refluxing benzene to $P(SiMe_3)_3$ and uncharacterized metal-containing products over ca. 1 day and a few hours, respectively. Compound **5** decomposed over 10–15 min in refluxing benzene primarily according to eq 4. Thus, the thermal-stability order in solution was **1** > **2** > **3** > **4** > **5**.

$$\tfrac{1}{2}[Pb[P(SiMe_3)_2]_2]_2 \xrightarrow{\Delta} Pb + (Me_3Si)_2PP(SiMe_3)_2 \quad (4)$$

The solution-phase decomposition of **6** was not studied, but because **6** was prepared (eq 2) in refluxing hexane, it is at least as thermally stable as **1** or **2**. When $Mn[N(SiMe_3)_2]_2(THF)$ and 2+ equiv of $HP(SiMe_3)_2$ were combined at room temperature instead of at reflux, the monosubstituted product $Mn[P(SiMe_3)_2][N(SiMe_3)_2]$ (**7**) was obtained instead of **6**. This contrasts with the syntheses of **1**–**5**, all of which were complete and, by necessity, conducted at room temperature or below. Extensive decomposition of **1**–**5** in *preparative* mixtures resulted unless lower reaction temperatures were maintained (see the Experimental Section), even though redissolved samples of *isolated* **1**–**5** had higher solution-phase stabilities. To summarize, **1**–**6** had sufficient thermal stability to be isolated but were less stable than the corresponding $N(SiMe_3)_2$ complexes.

Solid-State Structures. Compounds **1**–**3**, **5**, and **6**·THF were characterized by single-crystal X-ray diffraction. Crystallographic data are recorded in Table II. Thermal ellipsoid plots of the molecular units are given in Figures 1–4. Selected distances and angles are compared in Table III and are more completely listed in the figure captions. Tables of positional parameters for **2**, **3**, **5**, and **6**·THF are provided in the supplementary material. The structure of **1** was briefly presented earlier,[17a] and the positional parameters and other details were provided in the supplementary material accompanying that communication. In the solid state, each of the characterized examples possesses a dimeric molecular structure based on I, having two terminal and two bridging

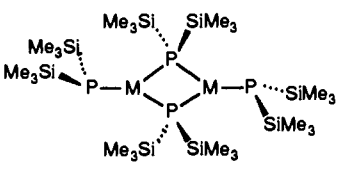

I

phosphido ligands. However, several distinctions between the various structures exist, and only the zinc and cadmium complexes **1** and **2** are strictly isostructural.

The molecular structure of **2** is shown in Figure 1 (a thermal ellipsoid plot of **1** was provided earlier[17a]). The dimeric units in

Table III. Comparisons of Distances and Angles in Disilylphosphido Complexes

	M				
param	Zn (**1**)	Cd (**2**)	Hg (**3**)	Pb (**5**)	Mn (**6**·THF)
M–P_t[a]	2.295 (1)	2.459 (1)	2.402 (1)[b]	2.70 (1)[c]	2.417 (2)[d]
					2.461 (2)[e]
M–P_b[a]	2.419 (1)	2.575 (1)	2.410 (1)[b]	2.77 (1)[c]	2.50 (1)[c,d]
	2.421 (1)	2.612 (1)	3.246 (1)		2.55 (1)[c,e]
P_t–M–P_b[a]	144.9 (1)	146.7 (1)	175.8 (1)	97.5 (4)[c]	144.8 (1)[d]
	124.1 (1)	124.3 (1)	95.0 (1)	111 (1)[c]	118.4 (1)[d]
					125.9 (1)[e]
					112.8 (1)[e]
P_b–M–P_b[a]	90.7 (1)	88.7 (1)	84.2 (1)	81.9 (5)[c]	96.8 (1)[d]
					94.1 (1)[e]
P_t–Si (av)[a]	2.226 (2)	2.222 (2)	2.232 (3)	2.24 (1)[c]	2.22 (1)[d]
					2.215 (3)[e]
P_b–Si (av)[a]	2.251 (2)	2.239 (2)	2.240 (3)	2.26 (1)[c]	2.242 (4)[c]
$\sum P_t$ angles[a]	316.8 (3)	311.4 (3)	308.2 (3)	299 (2)[c]	334.2 (3)[d]
					331.2 (3)[e]
Si–P_t–Si[a]	106.2 (1)	106.6 (1)	107.2 (1)	100.3 (4)[c]	106.6 (1)[d]
					105.1 (1)[e]
Si–P_b–Si[a]	107.0 (1)	108.2 (1)	107.3 (1)	109 (1)[c]	108.6 (1)[c]

[a] Distances are in angstroms; angles are in degrees; t = terminal, b = bridging. [b] "Bridges" in **3** result from weak secondary interactions; see text. [c] The two terminal or the two bridging ligands are not crystallographically equivalent; the value given is an average. [d] Value corresponds to the 3-coordinate Mn(1) center; see Figure 4. [e] Value corresponds to the 4-coordinate Mn(2) center; see Figure 4.

1 and **2** are centered on crystallographic inversion centers. The geometry about the metal atoms is distorted trigonal planar; the metal and phosphorus atoms are coplanar, but the P–M–P angles are not mutually equal to 120°. As expected, the intra-ring P_b–M–P_b angles (b = bridging) of ca. 90° are smaller than the ideal value of 120°. Because the phosphido ligands in **1** and **2** bridge nearly symmetrically and *all* the intra-ring angles are close to 90°, the central $M_2(\mu\text{-}P_b)_2$ units are nearly square.

The two P_t–M–P_b angles (t = terminal) at each M are unequal; one is close to the 120° ideal, and the other is ca. 20° larger. The expanded angles apparently result from the steric interaction of the $SiMe_3$ groups on each bridging ligand with the $SiMe_3$ groups on one of the two terminal ligands (see Figure 1). These interactions are induced by the pyramidal geometries of the terminal ligands. In each of **1**–**3**, **5**, and **6**·THF, the terminal $P(SiMe_3)_2$ ligands adopt distinctly pyramidal geometries, as quantified by the sums of the bond angles about P_t ($\sum P_t$ angles in Table III). In **1** and **2**, the M–P_b distances are ca. 0.1 Å longer than the M–P_t distances.

In the solid-state structure of **3** (see Figure 2), the $M[P(SiMe_3)_2]_2$ units are also associated in a pairwise fashion about

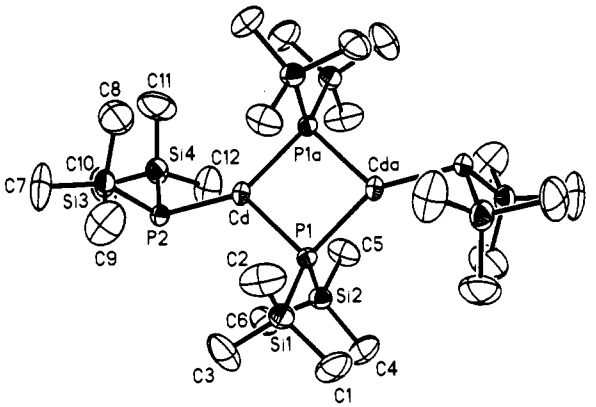

Figure 1. Thermal ellipsoid plot (20% probability contours) of $\{Cd[P(SiMe_3)_2]_2\}_2$ (**2**). Hydrogen atoms were omitted for clarity. Selected bond lengths and bond angles are given in Table III. $\{Zn[P(SiMe_3)_2]_2\}_2$ (**1**) and **2** are isostructural.

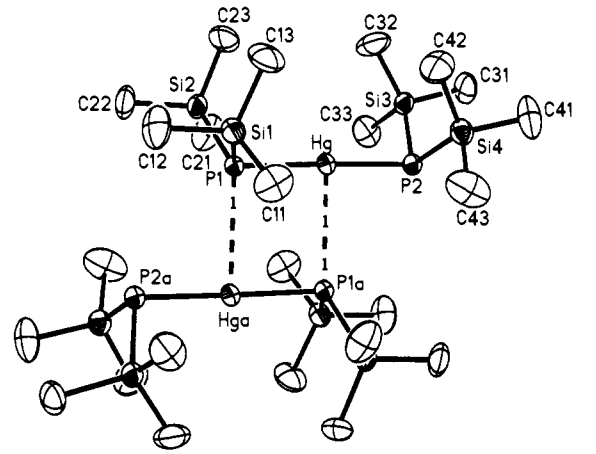

Figure 2. Thermal ellipsoid plot (20% probability contours) of $\{Hg[P(SiMe_3)_2]_2\}_2$ (**3**). Hydrogen atoms were omitted for clarity. Selected bond lengths and bond angles are given in Table III.

a crystallographic inversion center; however, in contrast to **1** and **2**, the phosphido bridges in **3** are extremely asymmetric. The longer Hg–P(1a) bridge distance of 3.246 (1) Å is only marginally shorter than the sum of the Hg and P van der Waals radii, 3.35 Å. We propose that the longer bridge separation corresponds to a secondary bond—a weak, dative interaction that does not disrupt the (linear) primary coordination geometry at Hg.[18] Thus, the $M–P_t$ and the shorter $M–P_b$ vectors, which represent the two primary covalent bonds in **3**, are approximately equal and essentially collinear. The overall geometry is T-shaped. NMR data suggest that **3** is monomeric in solution (see below), and so the secondary interactions apparently exist only in the solid state.

The homologous compound $Hg[P\text{-}t\text{-}Bu_2]_2$ was recently described as having a 2-coordinate linear geometry in the solid state with the P-*t*-Bu_2 ligands adopting an eclipsed conformation.[9a] In **3**, the terminal and bridging phosphido ligands also adopt an eclipsed conformation, which appears to be a steric minimum for the dimer (see Figure 2). When we examined a packing diagram for $Hg[P\text{-}t\text{-}Bu_2]_2$ generated from the supplementary data accompanying the earlier report,[9a] we found that **3** and $\{Hg[P\text{-}t\text{-}Bu_2]_2\}_2$ are actually isostructural dimers in the solid state, and so the origin of the eclipsing is the same for both cases. The long Hg–P(2a) bridge distance in $\{Hg[P\text{-}t\text{-}Bu_2]_2\}_2$ is 3.16 Å; this is shorter than the corresponding distance in **3** and is additional support for secondary bonding in the solid-state structures.

The molecular structure of the lead dimer **5** is shown in Figure 3. The 3-coordinate lead atoms have trigonal-pyramidal con-

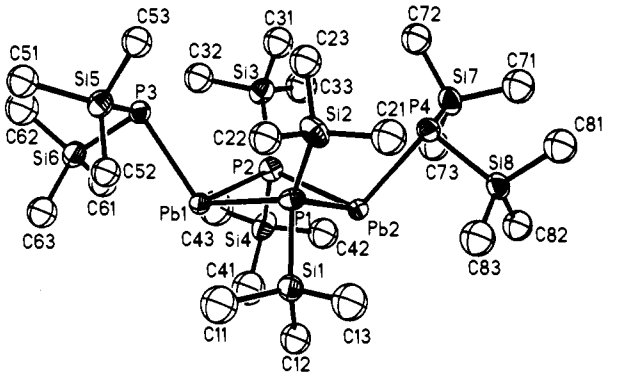

Figure 3. Thermal ellipsoid plot (20% probability contours) of $\{Pb[P(SiMe_3)_2]_2\}_2$ (**5**). Hydrogen atoms were omitted for clarity. Selected bond distances (Å): Pb(1)–P(1), 2.747 (7); Pb(1)–P(2), 2.774 (7); Pb(1)–P(3), 2.696 (7); Pb(2)–P(1), 2.796 (7); Pb(2)–P(2), 2.777 (7); Pb(2)–P(4), 2.696 (7); P(1)–Si(1), 2.264 (9); P(1)–Si(2), 2.270 (10); P(2)–Si(3), 2.256 (10); P(2)–Si(4), 2.263 (10); P(3)–Si(5), 2.261 (10); P(3)–Si(6), 2.241 (10); P(4)–Si(7), 2.237 (11); P(4)–Si(8), 2.235 (11). Selected angles (deg): P(1)–Pb(1)–P(2), 82.4 (2); P(1)–Pb(1)–P(3), 111.7 (2); P(2)–Pb(1)–P(3), 97.1 (2); P(1)–Pb(2)–P(2), 81.4 (2); P(1)–Pb(2)–P(4), 97.8 (2); P(2)–Pb(2)–P(4), 109.7 (2); Si(1)–P(1)–Si(2), 108.2 (4); Si(3)–P(2)–Si(4), 109.9 (4); Si(5)–P(3)–Si(6), 100.2 (4); Si(7)–P(4)–Si(8), 100.4 (4).

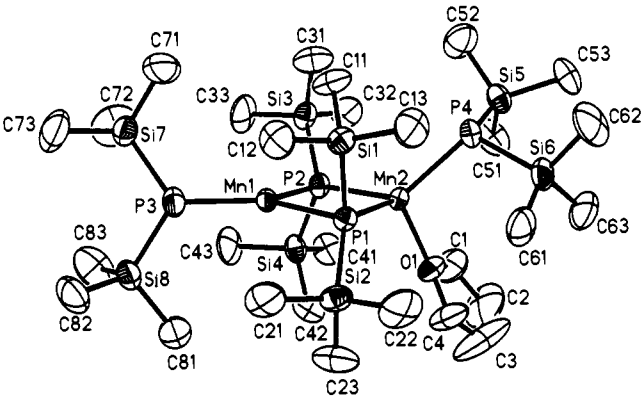

Figure 4. Thermal ellipsoid plot (20% probability contours) of $\{Mn[P(SiMe_3)_2]_2\}_2(THF)$ (**6**·THF). Hydrogen atoms were omitted for clarity. Selected bond distances (Å): Mn(1)–P(1), 2.493 (2); Mn(1)–P(2), 2.504 (2); Mn(1)–P(3), 2.417 (3); Mn(2)–P(1), 2.541 (2); Mn(2)–P(2), 2.565 (2); Mn(2)–P(4), 2.461 (2); Mn(2)–O(1), 2.163 (4); P(1)–Si(1), 2.246 (2); P(1)–Si(2), 2.238 (2); P(2)–Si(3), 2.241 (2); P(2)–Si(4), 2.241 (3); P(3)–Si(7), 2.211 (3); P(3)–Si(8), 2.227 (3); P(4)–Si(5), 2.216 (3); P(4)–Si(6), 2.214 (2). Selected angles (deg): P(1)–Mn(1)–P(2), 96.8 (1); P(1)–Mn(1)–P(3), 118.4 (1); P(2)–Mn(1)–P(3), 144.8 (1); P(1)–Mn(2)–P(2), 94.1 (1); P(1)–Mn(2)–P(4), 112.8 (1); P(2)–Mn(2)–P(4), 125.9 (1); Si(1)–P(1)–Si(2), 108.6 (1); Si(3)–P(2)–Si(4), 108.6 (1); Si(7)–P(3)–Si(8), 106.6 (1); Si(5)–P(4)–Si(6), 105.1 (1).

figurations as a result of stereochemically active metal-centered lone pairs. Thus, cis and trans isomers are possible (see II and

P = $P(SiMe_3)_2$
M = Sn (**4**), Pb (**5**)

III), and both are observed in solution (see below). **5** crystallizes as the cis isomer (II). The central $Pb_2(\mu\text{-}P_b)_2$ ring has a puckered rather than a planar geometry; all $Pb–P_b$ distances are approximately equal. As in **1** and **2**, the $M–P_b$ separations are ca. 0.1 Å longer than the $M–P_t$ separations. Cowley, Jones, and coworkers recently prepared the homologous compound $\{Pb[P\text{-}t\text{-}Bu_2]_2\}_2$;[9c] its solid-state structure is similar to that of **5** except that it crystallizes as the trans isomer (III) and has a planar central $Pb_2(\mu\text{-}P_b)_2$ ring.

(18) (a) Alcock, N. W. *Adv. Inorg. Chem. Radiochem.* **1972**, *15*, 1. (b) Sawyer, J. F.; Gillespie, R. J. *Prog. Inorg. Chem.* **1986**, *34*, 65. (c) Goel, S. C.; Chiang, M. Y.; Buhro, W. E. *J. Am. Chem. Soc.* **1990**, *112*, 6724.

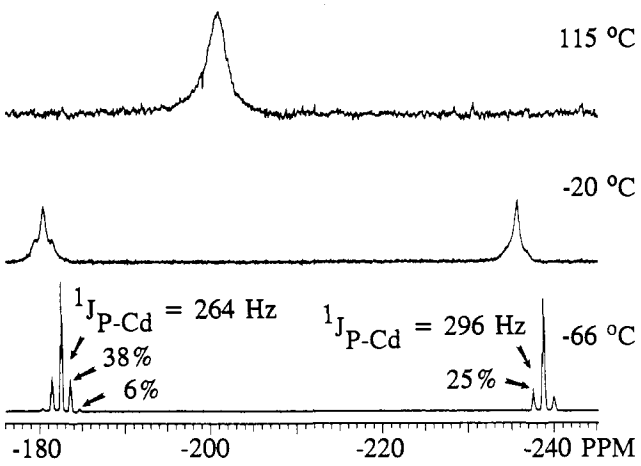

Figure 5. Variable-temperature $^{31}P\{^1H\}$ NMR spectra of $\{Cd[P(SiMe_3)_2][\mu\text{-}P(SiMe_3)_2]\}_2$ (2). The satellites (and their intensities) due to $^1J_{P-Cd}$ coupling are indicated by arrows; P-^{111}Cd and P-^{113}Cd couplings are unresolved. Values for $^1J_{P-Cd}$ coupling constants are also given.

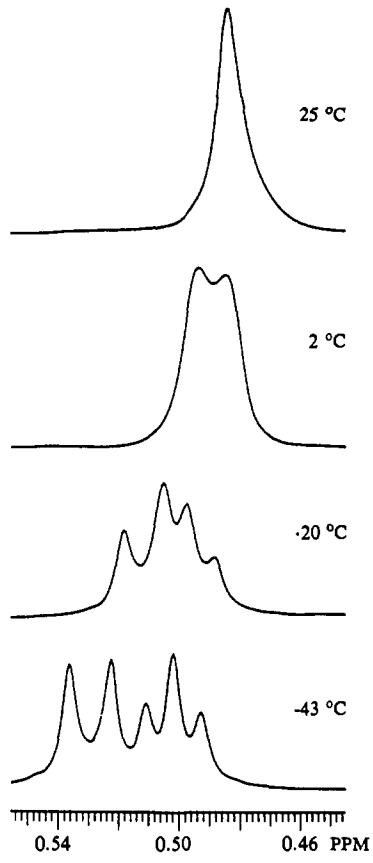

Figure 6. Variable-temperature ^1H NMR spectra of $\{Zn[P(SiMe_3)_2][\mu\text{-}P(SiMe_3)_2]\}_2$ (1). The doublet in the low-temperature-limit spectrum is assigned to the terminal $P(SiMe_3)_2$ ligands, and the virtual triplet is assigned to the bridging $P(SiMe_3)_2$ ligands; see text.

The manganese dimer 6·THF contains one 3- and one 4-coordinate manganese center (see Figure 4). The 3-coordinate Mn(1) has a distorted trigonal-planar geometry analogous to those of the metal atoms in 1 and 2. THF ligation produces a pseudotetrahedral environment at Mn(2) but does not greatly affect other aspects of the structure. For example, the Mn–P distances at the 4-coordinate Mn(2) are only ca. 0.05 Å longer than the corresponding distances for the 3-coordinate Mn(1). The central $Mn_2(\mu\text{-}P_b)_2$ ring is virtually planar; the mean deviation from the corresponding least-squares plane is 0.0261 Å. The Mn(2)–O(1) separation of 2.163 (4) Å is in the range of 2.15–2.20 Å observed in the $[Mn(H_2O)_6]^{2+}$ ion[19] and is therefore normal.

Bond distances and angles for the disilylphosphido complexes are summarized and compared in Table III. Two trends are apparent. First, the $M\text{–}P_t$ distances are in general accord with the sums of the covalent and/or Bragg–Slater M and P radii and are therefore consistent with $M\text{–}P_t$ single bonds. (The $M\text{–}P_b$ distances are longer than the $M\text{–}P_t$ distances as a result of their dative-bond component.[20]) Second, the sums of the angles about P_t ($\sum$ of P_t angles in Table III) correlate with the Pauling electronegativities of M. The largest sum (334°) corresponds to the most electropositive (Mn), the smallest sum (299°) corresponds to the least electropositive (Pb), and the intermediate cases fall in order. We believe that this slight trend toward ligand planarization with increasing Pauling electronegativity of the metal results from increasing ionic character in the M–P bonds. Increased ionic character should shorten the M–P single bonds and thereby induce the observed configurational flattening to relieve increased steric interactions between the P substituents. The P configurations remain distinctly pyramidal even for the most-flattened example (6·THF, $\sum P_t$ angles = 344°), and there is no justification to invoke π donation from P to M to account for the observed configurational trend.

Solution-Phase Structures and Dynamics. Compounds 1 and 2 exhibit fluxional behavior in solution. Their NMR data are similar and, at low temperature, are consistent with the dimeric solid-state structures described above. Thus, the low-temperature-limit $^{31}P\{^1H\}$ NMR spectra for 1 and 2 (see the Experimental Section) contain separate resonances for the bridging and terminal disilylphosphido ligands, which are triplets as a result of $^2J_{P-P}$ coupling. The variable-temperature data for the cadmium derivative 2 are presented in Figure 5. The resonances in the low-temperature spectrum of 2 possess ^{111,113}Cd (unresolved) satellites, which allow bridging and terminal assignments. The low-field resonance has two sets of satellites with intensities corresponding to the bridging ligands in the Cd–Cd* (38% abundant) and Cd*–Cd* (6% abundant) isotopomers. The high-field resonance has a single set of satellites with an intensity corresponding to the terminal ligands in both the Cd–Cd* and the Cd*–Cd* isotopomers. Similarly, we surmise that the low- and high-field resonances for 1 may also be assigned to the bridging and terminal ligands, respectively.

$^{31}P\{^1H\}$ NMR spectra recorded at higher temperatures reveal broadening and then coalescence of the resonances in 1 and 2 as a result of bridging-to-terminal site exchange (see Figure 6). The barriers calculated at the coalescence points are ΔG^*_{360} = 14.3 (2) kcal/mol and ΔG^*_{321} = 12.7 (6) kcal/mol for 1 and 2, respectively. The bridging-to-terminal site exchange is also evident by variable-temperature ^1H NMR spectroscopy, and the data for 1 are shown in Figure 6. The barriers calculated at the ^1H NMR coalescence points are ΔG^*_{281} = 14.8 (1) kcal/mol and ΔG^*_{246} = 12.4 (1) kcal/mol for 1 and 2, respectively. Note that the low-temperature-limit ^1H spectra for 1 and 2 each contain a doublet and a virtual triplet as a result of proton–phosphorus coupling (see Figure 6). Because the virtual-coupling pathway between the bridging ligands encompasses four bonds whereas the virtual-coupling pathway between the terminal ligands encompasses five bonds, we assign the virtual triplets to the $SiMe_3$ groups on the bridging ligands.

We propose that the mechanism(s) of bridging-to-terminal site exchange is (are) dissociative. Associative pathways would require unfavorable pyramidal coordination geometries about the metal atoms in 1 and 2. Dissociative pathways could proceed either by complete dissociation of the dimers into monomers and then reassociation (path a, Scheme I) or by cleavage of one M–P bridge bond, rotation about the remaining bridge bond, and then reclosure (path b, Scheme I). Paths a and b (Scheme I) were recently proposed by Westerhausen to account for the analogous behavior of the isostructural disilyl*amido* dimers $\{M[N(SiMe_3)_2]_2\}_2$ (M = Mg, Ca, Sr),[4d] and our data do not distinguish between them.

(19) Chiswell, B.; McKenzie, E. D.; Lindoy, L. F. In *Comprehensive Coordination Chemistry*; Wilkinson, G., Gillard, R. D., McCleverty, J. A., Eds.; Pergamon: New York, 1987; Vol. 4, Chapter 41, p 3.
(20) Haaland, A. *Angew. Chem., Int. Ed. Engl.* **1989**, *28*, 992.

Scheme I

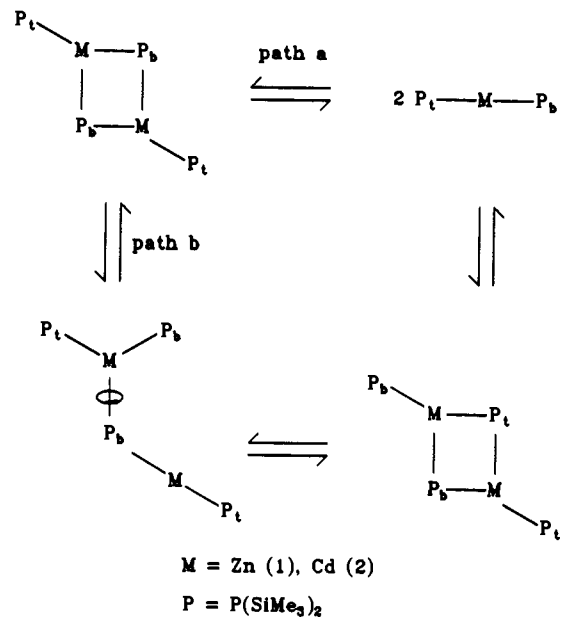

The NMR data for the analogous mercury compound **3** were consistent with a monomeric solution-phase structure. Both ^1H and $^{31}P\{^1H\}$ NMR spectra for **3** contained a single resonance and were temperature invariant in the range −78 to +70 °C (decomposition of **3** ensued above ca. +30 °C; see above). Although a dimeric structure similar to **1** and **2** undergoing very rapid bridging-to-terminal ligand exchange is not ruled out, it seems unlikely in view of the magnitudes of the site-exchange barriers established for **1** and **2** (see above). Note also that the dimeric structure adopted in the solid state results from very weak bridging interactions (see above); such secondary bonds are not expected to be maintained in solution.[18]

The tin (**4**) and lead (**5**) disilylphosphido complexes existed as equilibrating mixtures of cis and trans isomers in solution. Thus, the $^{31}P\{^1H\}$ NMR spectra contained two sets of resonances for both **4** and **5** (see Table I), in ratios of ca. 2:1 and 1:1, respectively, at room temperature. Bridging and terminal ligand resonances were assigned according to satellite intensities as for **1** and **2** above. The assignment of the resonances to cis and trans isomers required both $^{31}P\{^1H\}$ *and* ^1H NMR data. The $SiMe_3$ groups on the bridging disilylphosphido ligands are inequivalent in the cis isomers but equivalent in the trans isomers; consequently, three resonances in the ^1H NMR spectra of **4** and **5** pertained to the cis isomers and two pertained to the trans isomers. The cis and trans assignments in Table I were made by comparing the intensities of the resonances in the ^1H NMR and $^{31}P\{^1H\}$ spectra. The data revealed that *cis*-**4** predominated over *trans*-**4** by ca. 2:1 at room temperature whereas *cis*-**5** and *trans*-**5** were present in nearly equal amounts (see Table I).

The cis- and trans-isomer populations varied smoothly with temperature and were measured over the ranges of ca. 20–80 °C for **4** and ca. −20 to +70 °C for **5**. Cis–trans isomerization was fast on the laboratory time scale but slow on the NMR time scale; significant exchange broadening was not observed over the temperature ranges studied. Bridging-to-terminal ligand exchange was also slow on the NMR time scale over the temperature ranges studied. Linear plots of ln {[cis]/[trans]} vs $1/T$ were obtained using $^{31}P\{^1H\}$ NMR spectroscopy for **4** and ^1H NMR spectroscopy for **5**. The thermodynamic quantities for the trans ⇄ cis equilibria calculated from the plots were $\Delta H = -1.8$ (1) kcal/mol and $\Delta S = -4.7$ (2) eu for **4** and $\Delta H = -1.4$ (1) kcal/mol and $\Delta S = -4.4$ (2) eu for **5**.

The thermodynamic data indicate that the cis and trans isomers of **4** and **5** are nearly isoenergetic and that the cis isomers are actually slightly favored, both enthalpically and entropically. In contrast, the analogous compounds $\{Sn[P\text{-}t\text{-}Bu_2]_2\}_2$[11c] and $\{Pb[P\text{-}t\text{-}Bu_2]_2\}_2$[9c] were shown to exist in solution exclusively as the trans isomers; no cis–trans equilibria were detected. Although the cis isomers of **4**, **5**, and their P-*t*-Bu_2 analogs would appear to be disfavored by transannular interactions between the bulky terminal PR_2 ligands, we note from Figure 3 that the 4-membered ring in **5** puckers in a manner that lessens this transannular interaction. Such a puckering in trans isomers would not lead to a net relief of steric interactions, and indeed *trans*-$\{Pb[P\text{-}t\text{-}Bu_2]_2\}_2$ contains a planar ring in the solid state.[9c] The other significant steric interactions are the eclipsing of the terminal PR_2 ligands with the R substituents on the bridging PR_2 ligands; perhaps these interactions are dominant and approximately equal in the cis and trans isomers of **4** and **5**, thus accounting for their near energetic degeneracy. The cis and trans isomers of the parent dimers $[Sn(\mu\text{-}H)H]_2$ and $[Pb(\mu\text{-}H)H]_2$ were also found to be nearly isoenergetic by a recent theoretical study (although the trans isomers were slightly favored),[21] and a cis–trans equilibrium was experimentally observed in a related system: $[Sn(\mu\text{-}Cl)NR_2]_2$ (where NR_2 = tetramethylpiperidyl).[22] We conclude that the near degeneracy of the cis and trans isomers of $[Sn(\mu\text{-}PR_2)(PR_2)]_2$ and $[Pb(\mu\text{-}PR_2)(PR_2)]_2$ should be expected, and the absence of the cis isomers of $[Sn(\mu\text{-}P\text{-}t\text{-}Bu_2)(P\text{-}t\text{-}Bu_2)]_2$[11c] and $[Pb(\mu\text{-}P\text{-}t\text{-}Bu_2)(P\text{-}t\text{-}Bu_2)]_2$[9c] may reflect large barriers to isomer interconversion.

The manganese compounds $\{Mn[P(SiMe_3)_2]_2\}_2$ (**6**) and $Mn[P(SiMe_3)_2][N(SiMe_3)_2]$ (**7**) are paramagnetic and were not characterized by NMR spectroscopy. Solution-phase magnetic-moment measurements by the Evans method yielded μ_{eff} = 3.33 (5) μ_B per Mn for **6** and μ_{eff} = 3.65 (5) μ_B per Mn for **7**. These values are considerably lower than the spin-only value for 5 unpaired electrons (5.92 μ_B) expected for high-spin Mn(II) compounds and are very similar to the solid-state value for the disilyl*amido* dimer $\{Mn[N(SiMe_3)_2]_2\}_2$ (3.26 μ_B).[5d] The lower-than-spin-only values are consistent with antiferromagnetically coupled metal centers, thus arguing against monomeric solution-phase structures for **6** and **7**. Presumably, **6** adopts the dimeric structure I (see above) in solution (which is related to the established solid-state structure of **6**·THF, see above). Presumably, **7** adopts the related dimeric structure $\{Mn[\mu\text{-}P(SiMe_3)_2][N(SiMe_3)_2]\}_2$ (in which the phosphido ligands are bridging and the amido ligands are terminal). Our proposed structure for **7** is based on the solid-state structure of an analog, $\{Mn[\mu\text{-}PMes_2][N(SiMe_3)_2]\}_2$, which was recently reported by Power and co-workers.[23] Interestingly, the solution-phase μ_{eff} of $\{Mn[\mu\text{-}PMes_2][N(SiMe_3)_2]\}_2$ was 5.91 μ_B,[23] matching the expected spin-only value and perhaps suggesting its dissociation to monomers in solution.

Discussion

Preparative Strategy. To our knowledge, the first $P(SiR_3)_2$ complex was $Ti(NMe_2)_3[P(SiMe_3)_2]$, reported by Bürger and Neese in 1970;[24] it was prepared by a nucleophilic-substitution reaction between $LiP(SiMe_3)_2$ and $Ti(NMe_2)_3Br$. Subsequently, other *heteroleptic* $P(SiMe_3)_2$ complexes have been studied extensively by Schäfer[15] and Weber,[16] and these complexes have also been prepared by nucleophilic displacements of anionic leaving groups X from $L_nM\text{–}X$ precursors by $LiP(SiMe_3)_2$. Most of the *homoleptic* dialkylphosphido complexes were obtained analogously from $LiPR_2$ and metal halides or pseudohalides.[8-12] However, we used a different substitution strategy for the preparation of neutral homoleptic $P(SiMe_3)_2$ complexes, shown in eq 2, to avoid the formation of "ate" complexes and potential complications arising from the ability of $LiPR_2$ reagents to serve as reducing agents.[8,25]

The synthesis we have employed (eq 2) is a proton-transfer reaction in which protons are transferred from $HP(SiMe_3)_2$ to

(21) Trinquier, G. *J. Am. Chem. Soc.* **1990**, *112*, 2130.
(22) Chorley, R. W.; Hitchcock, P. B.; Jolly, B. S.; Lappert, M. F.; Lawless, G. A. *J. Chem. Soc., Chem. Commun.* **1991**, 1302.
(23) Chen, H.; Olmstead, M. M.; Pestana, D. C.; Power, P. P. *Inorg. Chem.* **1991**, *30*, 1783.
(24) Bürger, H.; Neese, H. J. *Inorg. Nucl. Chem. Lett.* **1970**, *6*, 299.
(25) Blake, P. C.; Hey, E.; Lappert, M. F.; Atwood, J. L.; Zhang, H. *J. Organomet. Chem.* **1988**, *353*, 307.

$N(SiMe_3)_2$ ligands. A few procedures analogous to eq 2 have been previously described. Bradley and co-workers reported that the lanthanide complexes $Ln[N(SiMe_3)_2]_3$ and $HPPh_2$ react according to eq 5 to give the partial substitution products $Ln[N(SiMe_3)_2]_2(PPh_2)$.[26] Power and co-workers reported that the transition metal disilylamido complexes $M[N(SiMe_3)_2]_2$ and $HPMes_2$ (Mes = mesityl) react according to eq 6 to give the partial substitution products $\{M[\mu\text{-}PMes_2][N(SiMe_3)_2]\}_2$.[23] Peringer found that $Hg[N(SiMe_3)_2]_2$ and HP-*t*-Bu_2 react according to eq 7 to give $Hg[P\text{-}t\text{-}Bu_2]_2$.[13d] We observed that the compounds

$$Ln[N(SiMe_3)_2]_3 + HPPh_2 \rightarrow Ln[N(SiMe_3)_2]_2(PPh_2) + HN(SiMe_3)_2 \quad (5)$$

Ln = La, Eu

$$M[N(SiMe_3)_2]_2 + HPMes_2 \rightarrow \tfrac{1}{2}\{M[N(SiMe_3)_2(\mu\text{-}PMes_2)]\}_2 + HN(SiMe_3)_2 \quad (6)$$

M = Mn, Fe

$$Hg[N(SiMe_3)_2]_2 + 2HP\text{-}t\text{-}Bu_2 \rightarrow Hg[P\text{-}t\text{-}Bu_2]_2 + 2HN(SiMe_3)_2 \quad (7)$$

$M[N(SiMe_3)_2]_2$ (M = Fe, Co) and $HP(SiMe_3)_2$ gave the partial substitution products $M[P(SiMe_3)_2][N(SiMe_3)_2]$ analogous to complex **7** and the examples by Bradley and Power.[27] (An incomplete crystal-structure determination of $Fe[P(SiMe_3)_2][N(SiMe_3)_2]$ revealed that it had the structure $\{Fe[\mu\text{-}P(SiMe_3)_2][N(SiMe_3)_2]\}_2$.[27]) Unlike complex **7**, the compounds $M[P(SiMe_3)_2][N(SiMe_3)_2]$ (M = Fe, Co) could not be converted to the homoleptic complexes $\{M[P(SiMe_3)_2]_2\}_2$ under more forcing conditions.

Structural Comparisons. A major goal of this work was to compare the structural properties of homologous disilylamido and disilylphosphido complexes. Two principal distinctions have emerged. (1) Terminal $P(SiMe_3)_2$ ligands have pyramidal configurations whereas terminal $N(SiMe_3)_2$ ligands have planar configurations. (2) The disilylphosphido complexes generally exhibit higher molecularities and higher coordination numbers about metal centers than do the corresponding disilylamido complexes. Both distinctions result from normal consequences of the established periodic relationships between N and P. We will argue that these periodic relationships govern the relative bridging tendencies of amido and phosphido ligands and, specifically, that the coordinating properties of amido ligands are a reflection of "the first-row anomaly".

Terminal amido or phosphido ligands may serve either as anionic 2-electron donors, in which the ligand lone pairs are localized on N or P, or as anionic 4-electron donors, in which the ligand lone pairs are delocalized to the metal and the M–N or M–P bonds have both σ and π components.[2,28] The pyramidal configurations and the single-bond M–P separations for the terminal $P(SiMe_3)_2$ ligands documented in Table III establish that the ligand lone pairs are localized on P. Consequently, the $P(SiMe_3)_2$ ligands in the homoleptic disilylphosphido complexes have no significant π-donor character.

Unlike terminal $P(SiMe_3)_2$ ligands, terminal $N(SiMe_3)_2$ ligands invariably exhibit planar configurations. However, despite their planar configurations, terminal $N(SiMe_3)_2$ ligands also do *not* possess significant π-donor character. Green and co-workers studied the photoelectron spectra of a series of disilylamido complexes, which indicated that M–N π bonding was minimal or nonexistent.[29] In a related study, Feldman and Calabrese reported organotitanium(III) complexes having planar NMePh ligands in which the π donation of N lone pairs to the titanium centers was unlikely or impossible.[30] In fact, the first example of a *pyramidal* terminal amido ligand (NHPh) was only recently discovered by Gladysz and co-workers.[31] An excellent discussion of the existing structural data on planar, 2-electron-donor amido ligands is given by Gladysz.[31b] Obviously, the planar configurations common to terminal amido ligands do not confirm the existence of N-to-M π bonding.

We attribute the planarity of 2-electron-donor (σ-only) amido ligands to the following characteristics of trivalent N.[32] (1) Steric interactions between the substituents on N (including the metal fragment) are significant because of the small size of N.[32] (2) First-row atoms readily engage in isovalent hybridization; consequently, N can easily achieve the sp^2 hybridization necessary to produce the planar configuration.[32] (3) Inversion barriers for trivalent N are low (4–8 kcal/mol in simple amines), reflecting the energetic accessibility of the planar configuration.[33] The steric environments about N atoms in $N(SiMe_3)_2$ (and other amido) ligands are very crowded, and planar configurations are thus the energetic minima. Others have emphasized the ability of the $N(SiMe_3)_2$ ligand to delocalize the N lone pair onto the $SiMe_3$ groups,[34] which may enforce the planar configuration. However, because terminal 2-electron-donor amido ligands are typically planar, whether they possess $SiMe_3$ substituents or not, any such N to Si delocalization is of secondary importance.[35]

The differing characteristics of trivalent P[32] compared to those of trivalent N account for the pyramidality of terminal 2-electron-donor $P(SiMe_3)_2$ ligands. Trivalent P is larger; therefore, steric interactions between substituents are less significant.[32] Unlike first-row atoms, second-row atoms do not engage in efficient isovalent hybridization;[32] thus, the sp^2 hybridization required for a planar P configuration is unfavorable. The unfavorability of the planar configuration is reflected in the high inversion barriers exhibited by trivalent P, which are ca. 30–40 kcal/mol, considerably higher than those for trivalent N.[33] Consequently, although neither $N(SiMe_3)_2$ nor $P(SiMe_3)_2$ ligands behave as π donors in their homoleptic complexes, the former have planar and the latter have pyramidal configurations. We will argue below that this difference in the configurational minima for the two ligands is an important factor governing their relative bridging tendencies.

In general, disilylphosphido complexes have higher degrees of association than do the corresponding disilylamido complexes. The compounds $M[N(SiMe_3)_2]_2$ are monomeric in the gas phase (M = Zn,[36] Cd,[37] Hg,[38] Sn,[39] Pb,[39] Mn[5d]), in solution (M = Zn,[1a] Cd,[1a] Hg,[1a] Sn,[40] Pb[40]), and in the solid state (M = Sn,[39] Pb[39]). $Mn[N(SiMe_3)_2]_2$ is dimeric in solution[5d] and in the solid state,[41] in which it has the structure $\{Mn[\mu\text{-}N(SiMe_3)_2][N(SiMe_3)_2]\}_2$ analogous to the disilylphosphido complexes reported here. The complex $Mn[N(SiMe_3)_2]_2$ also exists as a monomeric, volatile adduct $Mn[N(SiMe_3)_2]_2(THF)$.[41] All of the corresponding $P(SiMe_3)_2$ complexes are dimeric in solution and in the solid state as reported above, except for the Hg compound **3** which is ap-

(26) Aspinall, H. C.; Bradley, D. C.; Sales, K. D. *J. Chem. Soc., Dalton Trans.* **1988**, 2211.
(27) Goel, S. C.; Kramer, K. S.; Chiang, M. Y.; Buhro, W. E., unpublished.
(28) Collman, J. P.; Hegedus, L. S.; Norton, J. R.; Finke, R. G. *Principles and Applications of Organotransition Metal Chemistry*; University Science Books: Mill Valley, CA, 1987; pp 72–78.
(29) Green, J. C.; Payne, M.; Seddon, E. A.; Andersen, R. A. *J. Chem. Soc., Dalton Trans.* **1982**, 887.
(30) Feldman, J.; Calabrese, J. C. *J. Chem. Soc., Chem. Commun.* **1991**, 1042.
(31) (a) Dewey, M. A.; Arif, A.; Gladysz, J. A. *J. Chem. Soc., Chem. Commun.* **1991**, 712. (b) Dewey, M. A.; Knight, A. D.; Arif, A. M.; Gladysz, J. A. *Chem. Ber.* **1992**, *125*, 815.
(32) Kutzelnigg, W. *Angew. Chem., Int. Ed. Engl.* **1984**, *23*, 272.
(33) Rauk, A.; Allen, L. C.; Mislow, K. *Angew. Chem., Int. Ed. Engl.* **1970**, *9*, 400.
(34) Reference 2, pp 244–249.
(35) See also the discussion by Hanusa, which relates N–Si distances and Si–N–Si angles to steric effects rather than to N-to-Si delocalization.[4g]
(36) Haaland, A.; Hedberg, K.; Power, P. P. *Inorg. Chem.* **1984**, *23*, 1972.
(37) Alyea, E. C.; Fisher, K. J.; Fjeldberg, T. *J. Mol. Struct.* **1985**, *127*, 325.
(38) Alyea, E. C.; Fisher, K. J.; Fjeldberg, T. *J. Mol. Struct.* **1985**, *130*, 263.
(39) Fjeldberg, T.; Hope, H.; Lappert, M. F.; Power, P. P.; Thorne, A. J. *J. Chem. Soc., Chem. Commun.* **1983**, 639.
(40) Gynane, M. J. S.; Harris, D. H.; Lappert, M. F.; Power, P. P.; Rivière, P.; Rivière-Baudet, M. *J. Chem. Soc., Dalton Trans.* **1977**, 2004.
(41) Bradley, D. C.; Hursthouse, M. B.; Malik, K. M. A.; Möseler, R. *Transition Met. Chem. (London)* **1978**, *3*, 253.

parently monomeric in solution. The dimeric association of the Mn complex **6** appears to be more robust than the dimeric association of $\{Mn[\mu\text{-}N(SiMe_3)_2][N(SiMe_3)_2]\}_2$ because the latter can be disrupted by adduct formation with THF whereas **6** forms a THF adduct with the dimeric structure intact (**6**·THF). Therefore, with the exceptions of M = Mn and Hg noted, the disilylphosphido complexes have higher molecularities than the disilylamido complexes. The higher degrees of aggregation for the disilylphosphido complexes correspond to higher coordination numbers about both M and P atoms.

The higher molecularities and higher P coordination numbers exhibited by the disilylphosphido complexes demonstrate clearly that $P(SiMe_3)_2$ ligands have stronger bridging tendencies than do $N(SiMe_3)_2$ ligands. This conclusion is expected. In general, the stronger bridging tendencies of phosphido ligands relative to the corresponding amido ligands are probably already widely accepted[42] on the basis of the following. Although bridging phosphido ligands are common, until recently, terminal phosphido ligands were rare.[28,42,43] In contrast, terminal amido ligands are common. The ability of amido ligands, especially $N(SiMe_3)_2$ ligands, to enforce low coordination numbers about metal centers and to maintain low degrees of aggregation by serving as stable terminal ligands is well-known.[2] However, to our knowledge, the stronger bridging tendencies of phosphido ligands relative to amido ligands have not been systematically confirmed. We believe that the present study, which compares a *series* of homologous binary amido and phosphido complexes, is the best available demonstration.

What factors are responsible for the stronger bridging tendency of phosphido ligands? Before stating our best rationalization, we will cite a few potential factors that appear to be excluded. Chisholm and co-workers recently showed that terminal amido ligands are stronger π donors than are terminal phosphido ligands;[44] consequently, amido ligands might be relatively stabilized in terminal positions by π bonding. However, in the present study, neither the terminal $N(SiMe_3)_2$ ligands nor the terminal $P(SiMe_3)_2$ ligands behave as π donors, yet the $P(SiMe_3)_2$ ligands exhibit a stronger bridging tendency. Gladysz and co-workers have suggested that the strong bridging tendency of phosphido ligands may be due to increased p character in the P lone pairs that results from the larger-than-normal bond angles (for trivalent P) in terminal, pyramidal, 2-electron-donor phosphido ligands.[45] However, Kutzelnigg has presented quantum-chemical arguments that the p character in the lone pairs of normal trivalent phosphorus compounds (bond angles = ca. 90–95°) is dramatically underestimated by the conventional geometric analysis of hybridization.[32] For example, the hybridization of the P lone pair in PH_3 (bond angles = 94°) is actually s:p = 1.05:1.00 whereas the conventional geometric analysis would predict ca. s:p = 4.35:1.00, or significantly less p character.[32] Consequently, the larger bond angles in terminal phosphido ligands probably do not induce the substantial increase in lone-pair p character formerly expected.[45] Finally, terminal phosphido ligands should serve as softer bases than terminal amido ligands, which might rationalize their stronger bridging tendencies in certain cases. However, the *weakest* $P(SiMe_3)_2$ bridge corresponded to the *softest* metal ion in our study, Hg^{2+} (compound **3**). Additionally, we found strong $P(SiMe_3)_2$ bridges in complexes of both soft metal ions and hard metal ions.[46] Consequently, HSAB theory does not provide the proper model for rationalizing the bridging properties of the ligands.

We suggest that phosphido ligands have stronger relative bridging tendencies for the same fundamental reasons that other properties of P and N differ. The most important factors that differentiate the properties of P and N are the larger size, lower electronegativity, and lower hybridization tendency of P.[32] For example, recent theoretical work has established that the ability of P to form hypervalent compounds, whereas N cannot, is primarily due to the larger size and lower electronegativity of P.[32,47] Because hypervalency and ligand bridging both involve coordination expansion about N or P, it is reasonable that they should be governed by similar factors. Furthermore, terminal 2-electron-donor phosphido ligands are configurationally prepared for bridge formation; their pyramidal equilibrium configurations are very close to the geometry required by the bridges. In contrast, the equilibrium planarity of terminal 2-electron-donor amido ligands requires that bond angles about N be compressed and, therefore, steric interactions among substituents be increased to accommodate bridge formation. To summarize, phosphido ligands are better bridging ligands primarily because the larger P is better able to adopt the higher coordination number; the distinction is principally a steric effect. Additionally, the longer M–P (as compared to M–N) distances provide less sterically encumbered environments for M atoms as well as P atoms.

The differing properties of amido and phosphido ligands can ultimately be attributed to the first-row anomaly. First-row (second-period) elements are anomalous because, unlike the heavier elements in the main group, they hybridize easily and efficiently, engage in strong multiple bonds, and exhibit only "normal" valencies (≤ 4).[32] Hybridization is used by first-row elements as a means of reducing steric interactions among substituents (Pauli repulsions), which are significant.[32] The hybridization behavior of trivalent N and the magnitude of the steric interactions make amido ligands poorer bridge formers. Such effects should be much less obvious in comparisons of alkoxide vs thiolate ligands or fluoride vs chloride ligands because these ligands have only one or no substituent, respectively. Consequently, amido ligands should be unique in exhibiting significantly weaker bridging tendencies than homologous ligands based on heavier congeners.

Experimental Section

General Methods. All ambient-pressure procedures were carried out under dry N_2 using standard inert-atmosphere techniques. The starting compounds $M[N(SiMe_3)_2]_2$ (M = Zn,[1a] Cd,[1a] Hg,[1a] Sn,[40] Pb[40]) and $Mn[N(SiMe_3)_2]_2(THF)$[41] were prepared according to literature procedures. $HP(SiMe_3)_2$ was prepared from $P(SiMe_3)_3$[48] as previously described.[49] Hexane, benzene, and toluene were distilled from sodium benzophenone ketyl. NMR solvents were sparged with N_2 and stored over type 4A sieves.

Melting points were measured under N_2. C, H, and N analyses were performed by Oneida Research Services, Whitesboro, NY. Zn, Cd, Pb, and Mn were determined by EDTA titrations.[50] Hg was estimated gravimetrically as HgS.[51] NMR probe temperatures were calibrated with methanol or ethylene glycol standards in variable-temperature experiments.

Preparation of $\{Zn[P(SiMe_3)_2]_2\}_2$ (1). $HP(SiMe_3)_2$ (3.31 mL, 2.71 g, 15.2 mmol) and $Zn[N(SiMe_3)_2]_2$ (2.95 g, 7.6 mmol) were combined in benzene (20 mL) at room temperature with stirring. The reaction mixture was transferred to a −5 °C refrigerator for 15 h whereupon white crystals of **1** were deposited. Crystalline **1** was collected by filtration, washed with cold benzene (2 mL), and dried. The mother liquor was concentrated to 7–8 mL and stored in a −5 °C refrigerator to give a second crop of crystalline **1**, which was collected as above to give a combined yield of 2.78 g (6.6 mmol, 87%). Mp: >250 °C; gradual darkening above 100 °C. Anal. Calcd for $C_{24}H_{72}P_4Si_8Zn_2$: C, 34.25; H, 8.64; N, 0; Zn, 15.56. Found: C, 32.54, 31.43, 29.59; H, 8.34, 8.03, 8.17; N, 0.00; Zn, 15.78. Note that the carbon analysis is outside the normally acceptable range.

(42) Bohra, R.; Hitchcock, P. B.; Lappert, M. F.; Leung, W.-P. *J. Chem. Soc., Chem. Commun.* **1989**, 728.
(43) Cotton, F. A.; Wilkinson, G. *Advanced Inorganic Chemistry*, 5th ed.; Wiley: New York, 1988; p 440.
(44) Buhro, W. E.; Chisholm, M. H.; Folting, K.; Huffman, J. C.; Martin, J. D.; Streib, W. E. *J. Am. Chem. Soc.* **1992**, *114*, 557.
(45) Buhro, W. E.; Zwick, B. D.; Georgiou, S.; Hutchinson, J. P.; Gladysz, J. A. *J. Am. Chem. Soc.* **1988**, *110*, 2427.
(46) Pearson, R. G. *Inorg. Chem.* **1988**, *27*, 734.
(47) (a) Reed, A. E.; Schleyer, P. v. R. *J. Am. Chem. Soc.* **1990**, *112*, 1434. (b) Reed, A. E.; Weinhold, F. *J. Am. Chem. Soc.* **1986**, *108*, 3586.
(48) Askham, F. R.; Stanley, G. C.; Marques, E. C. *J. Am. Chem. Soc.* **1985**, *107*, 7423.
(49) Bürger, H.; Goetze, U. *J. Organomet. Chem.* **1968**, *12*, 451.
(50) Basset, J.; Denney, R. C.; Jeffery, G. H.; Mendham, J. *Vogel's Textbook of Quantitative Inorganic Analysis*, 4th ed.; Wiley: New York, 1978; pp 324–325.
(51) Reference 50, pp 470–471.

Compound **1** was soluble in hexane, benzene, and toluene. **1** (0.38 g, 0.90 mmol) sublimed (10^{-4} Torr, 140 °C bath) to give **1** as a crystalline solid (0.20 g, 0.48 mmol, 53%).

Preparation of $\{Cd[P(SiMe_3)_2]_2\}_2$ (2). $HP(SiMe_3)_2$ (3.58 mL, 2.93 g, 16.5 mmol) and $Cd[N(SiMe_3)_2]_2$ (3.57 g, 8.24 mmol) were combined in cold benzene (25 mL). The mixture was stirred for 0.5 h in an ice bath, and then the volume was reduced to 15 mL. The reaction flask was transferred to a −5 °C refrigerator for 12 h whereupon pale-yellow crystals of **2** formed. The first crop of crystals was collected by filtration, washed with 2 mL of cold benzene, and dried. The mother liquor was concentrated to 7–8 mL, and a second crop of **2** was similarly obtained for a total yield of 3.50 g (7.5 mmol, 90%). Mp: 214–215 °C dec; gradual darkening above 126 °C. Anal. Calcd for $C_{24}H_{72}Cd_2P_4Si_8$: C, 30.85; H, 7.77; Cd, 24.06; N, 0. Found: C, 30.28; H, 7.44; Cd, 23.89; N, 0.05.

Compound **2** was soluble in hexane, benzene, and toluene. **2** (0.16 g, 0.35 mmol) sublimed (10^{-4} Torr, 140 °C bath) to give **2** as a light-yellow crystalline solid (0.12 g, 0.26 mmol, 75%).

Preparation of $Hg[P(SiMe_3)_2]_2$ (3). A hexane (50 mL) solution of $Hg[N(SiMe_3)_2]_2$ (5.36 g, 10.3 mmol) was cooled to −12 °C in an ice–acetone bath, and $HP(SiMe_3)_2$ (4.50 mL, 3.68 g, 20.7 mmol) was added slowly by syringe over 6–7 min with stirring. After 0.5 h, the solution was transferred to a −20 °C freezer for 15 h. Colorless crystals of **3** formed and were collected by filtration, washed with 2 mL of cold hexane, and dried. A second crop of crystals was obtained similarly from the filtrate after it was concentrated to ca. 15 mL. The total yield of **3** was 4.65 g, 8.4 mmol, 82%. Mp: 90–91 °C dec. Anal. Calcd for $C_{12}H_{36}HgP_2Si_4$: C, 25.96; H, 6.53; Hg, 36.12; N, 0. Found: C, 26.04; H, 6.15; Hg, 35.78; N, 0.00.

Compound **3** was soluble in hexane, benzene, and toluene. Crystalline **3** was unstable at room temperature but was stored at −20 °C for several months without decomposition. Benzene solutions of **3** were stable for a few days at room temperature but decomposed slowly over ca. 1 mo to $P(SiMe_3)_3$, trace amounts of $(Me_3Si)_2PP(SiMe_3)_2$,[52] and an uncharacterized brown precipitate. Benzene solutions of **3** heated to 65–80 °C decomposed similarly over ca. 1 day.

Preparation of $\{Sn[P(SiMe_3)_2]_2\}_2$ (4). $HP(SiMe_3)_2$ (2.20 mL, 1.80 g, 4.6 mmol) and $Sn[N(SiMe_3)_2]_2$ (2.00 g, 5.0 mmol) were combined in hexane (15 mL) at −20 °C with stirring. The resulting mixture was transferred to a −20 °C freezer for 15 h whereupon red-orange crystals of **4** formed. After the mother liquor was removed by cannula, the crystals were washed with 1 mL of cold hexane and dried (1.60 g, 3.4 mmol, 68%). Mp: 129–130 °C dec. Anal. Calcd for $C_{24}H_{72}P_4Si_8Sn_2$: C, 30.44; H, 7.66; N, 0. Found: C, 30.23; H, 7.53; N, 0.00.

4 was soluble in hexane, benzene, and toluene. Crystalline **4** decomposed over several months at room temperature but was stored for >6 mo without detectable decomposition in a −20 °C freezer. In refluxing benzene, **4** decomposed in a few hours to $P(SiMe_3)_3$ as the major P-containing product and other unidentified soluble species.

Preparation of $\{Pb[P(SiMe_3)_2]_2\}_2$ (5). A hexane (15 mL) solution of $Pb[N(SiMe_3)_2]_2$ (1.54 g, 2.9 mmol) was cooled to −10 °C in an ice–acetone bath, and $HP(SiMe_3)_2$ (1.27 mL, 1.04 g, 5.8 mmol) was added with stirring. The resulting mixture was then transferred to a −20 °C freezer for 15 h whereupon dark-red crystals of **5** formed. After the mother liquor was removed by cannula, the crystals were washed with 2 mL of cold hexane and dried under vacuum (1.25 g, 2.2 mmol, 77%). Mp: 94–95 °C dec. Anal. Calcd for $C_{24}H_{72}P_4Pb_2Si_8$: C, 25.66; H, 6.46; N, 0; Pb, 36.89. Found: C, 25.58; H, 6.38; N, 0.00; Pb, 36.65.

Compound **5** was soluble in hexane, benzene, and toluene. Crystalline **5** was not stable at room temperature for extended periods and was routinely stored in a −20 °C freezer. In refluxing benzene, **5** decomposed within 10–15 min to $(Me_3Si)_2PP(SiMe_3)_2$ (ca. 80%),[52] $P(SiMe_3)_3$ (ca. 20%), and lead metal (identified by XRD).

Preparation of $\{Mn[P(SiMe_3)_2]_2\}_2(THF)$ (6·THF). $HP(SiMe_3)_2$ (1.50 mL, 1.23 g, 6.88 mmol) and $Mn[N(SiMe_3)_2]_2(THF)$ (1.50 g, 3.35 mmol) were combined in hexane (20 mL). The resulting mixture was refluxed for 6 h and then allowed to cool slowly to room temperature whereupon dark-purple, needle-shaped crystals of **6**·THF formed. After the mother liquor was removed by cannula, the crystals were washed with 1 mL of hexane. Vacuum drying gave a sticky solid resulting from loss of the THF solvate (0.80 g, 2.37 mmol, 70% based on $\{Mn[P(SiMe_3)_2]_2\}_2$ (**6**)). Anal. Calcd for $\{Mn[P(SiMe_3)_2]_2\}_2$, $C_{24}H_{72}Mn_2P_4Si_8$: C, 35.18; H, 8.85; Mn, 13.41; N, 0. Calcd for $\{Mn[P(SiMe_3)_2]_2\}_2(THF)$, $C_{24}H_{72}Mn_2P_4Si_8 \cdot C_4H_8O$: C, 37.72; H, 9.05; Mn, 12.32; N, 0. Found: C, 36.02; H, 8.94; Mn, 13.70; N, 0.01. Note that the carbon determination was between the theoretical values for the solvated and the unsolvated formulas, but the composite analyses were most consistent with the unsolvated formula. Magnetic moment (of unsolvated **6**): μ_{eff} = 3.33 (5) μ_B per Mn (determined by the Evans method in toluene, room temperature).

Compound **6** was soluble in hexane, benzene, and toluene and decomposed upon attempted sublimation.

Preparation of $Mn[P(SiMe_3)_2][N(SiMe_3)_2]$ (7). $Mn[N(SiMe_3)_2]_2$·(THF) (1.66 g, 3.7 mmol) and $HP(SiMe_3)_2$ (1.92 mL, 1.57 g, 8.8 mmol) were combined in hexane (20 mL) with stirring at room temperature. The color of solution changed from purple to dark red in ca. 15 min. Stirring was continued for 15 h, and then the volume of the solution was reduced to 7–8 mL. The reaction vessel was transferred to a −20 °C freezer for 15 h whereupon dark-purple crystals of **7** formed. The mother liquor was removed by cannula, and the crystals were washed with 1 mL of hexane and dried under vacuum (1.30 g, 3.31 mmol, 89%). Mp: 222–223 °C. Anal. Calcd for $C_{12}H_{36}MnNPSi_4$: C, 36.70; H, 9.24; N, 3.56; Mn, 13.99. Found: C, 36.99; H, 9.13; N, 3.52; Mn, 13.73. IR (cm^{-1}, KBr): 2955 m, 2899 w, 1384 w, 1244 s, 1181 vw, 1061 w, 991 m, 843 vs, 752 w, 672 vw, 625 w, 459 vw. Magnetic moment: μ_{eff} = 3.65 (5) μ_B per Mn (determined by the Evans method in toluene, room temperature).

Compound **7** was soluble in hexane, benzene, and toluene, and **7** (0.40 g, 1.02 mmol) sublimed (10^{-4} Torr, 140 °C bath) to give dark-purple crystals (0.22 g, 0.56 mmol, 56%).

Thermal Decomposition of $\{Zn[P(SiMe_3)_2]_2\}_2$ (1). A toluene solution (20 mL) of **1** (0.90 g, 2.1 mmol) was brought to reflux. Within 2–3 h, a yellow precipitate began to form. The course of the reaction was periodically monitored by ^{31}P NMR, which indicated $P(SiMe_3)_3$ was the only soluble P-containing product. All of **1** was consumed after 7 days. The yellow precipitate, $[ZnP(SiMe_3)]_x$, was collected by filtration, washed with benzene (3 × 25 mL), and dried under vacuum (0.29 g, 1.7 mmol, 81%). Mp: >250 °C. Anal. Calcd for C_3H_9PSiZn: C, 21.25; H, 5.35; N, 0; Zn, 38.56. Found: C, 21.13; H, 5.26; N, 0.21; Zn, 38.46. IR (cm^{-1}, KBr): 2947 m, 2890 m, 1441 w, 1398 m, ν_{Si-Me} 1239 s, 1095 w, 1023 w, ν_{Si-Me} 828 vs, 745 m, 686 m, 628 s, 454 s. $[ZnP(SiMe_3)]_x$ was insoluble in hydrocarbons, pyridine, and DME.

Thermal Decomposition of $\{Cd[P(SiMe_3)_2]_2\}_2$ (2). A toluene solution (25 mL) of **2** (1.30 g, 2.8 mmol) was refluxed for 5 days. Within 1–2 h, a light-green precipitate began to form. The precipitate, $[CdP(SiMe_3)]_x$, was collected by filtration, washed with benzene (10 mL), and dried under vacuum (0.50 g, 2.3 mmol, 83%). Mp: >250 °C. Anal. Calcd for C_3H_9CdPSi: C, 16.63; H, 3.72; Cd, 51.91; N, 0. Found: C, 17.02; H, 3.81; Cd, 52.16; N, 0.00. IR (cm^{-1}, KBr): 2945 w, 2889 vw, 1385 w, ν_{Si-Me} 1239 m, 1060 vw, ν_{Si-Me} 829 vs, 744 vw, 684 w, 627 m, 453 m. $[CdP(SiMe_3)]_x$ was insoluble in hydrocarbons, pyridine, and DME.

NMR Studies of the Dynamic Behavior of 1 and 2. Rate constants and ΔG^* values and error estimates were extracted from the data by standard methods.[53] Data for **1**: ^1H NMR (δ, toluene-d_8, −43 °C, low-temperature limit) 0.53 (d, $^3J_{H-P}$ = 4.2 Hz, 36 H), 0.52 (virtual t, $^{3,5}J_{H-P}$ = 2.7 Hz, 36 H); T_c = 281 (2) K; $\Delta\nu$ = 8.32 (100) Hz; rate constant k_{281} = 18.5 (2.2) s^{-1}; ΔG^*_{281} = 14.8 (1) kcal/mol; $^{31}P\{^1H\}$ NMR (ppm, toluene-d_8, −48 °C, low-temperature limit) −186.0 (t, $^2J_{P-P}$ = 24.8 Hz), −241.5 (t, $^2J_{P-P}$ = 24.8 Hz); T_c = 360 (5) K; $\Delta\nu$ = 6741 (25) Hz; rate constant k_{360} = 14 975 (60) s^{-1}; ΔG^*_{360} = 14.3 (2) kcal/mol. Data for **2**: ^1H NMR (δ, toluene-d_8, −66 °C, low-temperature limit) 0.55 (d, $^3J_{H-P}$ = 4.0 Hz, 36 H), 0.47 (virtual t, $^{3,5}J_{H-P}$ = 2.6 Hz, 36 H); T_c = 246 (2) K; $\Delta\nu$ = 22.84 (100) Hz; rate constant k_{246} = 50.7 (2.2) s^{-1}; ΔG^*_{246} = 12.4 (1) kcal/mol; $^{31}P\{^1H\}$ NMR (ppm, toluene-d_8, −66 °C, low-temperature limit) −182.9 (t, $^2J_{P-P}$ = 16.1 Hz; satellites $^1J_{P-Cd}$ = 264 Hz, intensities = 6% for Cd*–Cd* and 38% for Cd–Cd* isotopomers; bridging), −239.4 (t, $^2J_{P-P}$ = 16.0 Hz; satellites $^1J_{P-Cd}$ = 296 Hz, intensity = 26% for Cd*–Cd* and Cd–Cd* isotopomers; terminal); T_c = 321 (15) K; $\Delta\nu$ = 6837 (60) Hz; rate constant k_{321} = 15 188 (133) s^{-1}; ΔG^*_{321} = 12.7 (6) kcal/mol.

Measurement of the Temperature Dependence of the Cis–Trans Equilibria of 4 and 5. Thermodynamic quantities were extracted by fitting the data to the following equation: $\ln\{[cis]/[trans]\} = -\Delta H/RT + \Delta S/R$. Errors were estimated by standard procedures.[54] Data for **4** were obtained by integrating $^{31}P\{^1H\}$ NMR resonances; data for **5** were obtained by integrating ^1H NMR resonances. Data for **4**: (K, [cis]/[trans]) 296, 2.03; 305, 1.79; 315, 1.62; 326, 1.46; 336, 1.39; 344, 1.27; 354, 1.23. Data for **5**: (K, [cis]/[trans]) 249, 1.86; 272, 1.56; 294, 1.27; 317, 1.08; 340, 0.85. The thermodynamic quantities determined from the plots of $\ln\{[cis]/[trans]\}$ vs $1/T$ were ΔH = −1.8 (1) kcal/mol and ΔS = −4.7 (2) eu for **4** and ΔH = −1.4 (1) kcal/mol and ΔS = −4.4 (2) eu for **5**.

(52) Schumann, H.; Fischer, R. *J. Organomet. Chem.* **1975**, *88*, C13.

(53) Sandström, J. *Dynamic NMR Spectroscopy*; Academic: New York, 1982.

(54) Bevington, P. R. *Data Reduction and Error Analysis for the Physical Sciences*; McGraw-Hill: New York, 1969; p 114.

Crystallographic Procedures. Crystalline samples suitable for diffraction analysis were obtained as follows. Colorless crystals of **1** were obtained from benzene solution at room temperature. Light-yellow crystals of **2** were obtained from the reaction mixture in benzene at 5 °C. Colorless crystals of **3** and dark-red crystals of **5** were obtained from the respective reaction mixtures at -20 °C. Dark-purple plates of **6**·THF were obtained from the reaction mixture in hexane at room temperature.

All samples were mounted in thin-wall glass capillaries in an inert-atmosphere glovebox. The intensity data for compounds **1**, **3**, and **5** were collected on a Siemens R3m/v diffractometer at ambient temperature. The data for **2** and **6** were collected on a Nicolet P3 diffractometer at ambient temperature. On both diffractometers, Mo Kα radiation (λ = 0.71073 Å) was used except in the case of **1** for which Cu Kα radiation was used (λ = 1.54178 Å).

Crystallographic calculations were done on a microVAX II using the Siemens SHELXTL PLUS program package. Crystal data are summarized in Table II. Neutral-atom scattering factors were used.[55] All structures were solved by direct methods. On the basis of systematic extinctions or lack of them, the space groups were assigned to be $P\bar{1}$ (No. 2) for **1**-**3**, and **6**, and $P2_12_12_1$ (No. 19) for **5**. Refinements for each are described in the supplementary material. All non-hydrogen atoms were refined anisotropically. All hydrogen atoms were placed in calculated positions (d_{C-H} = 0.96 Å) and included in the final structure factor calculations by using a riding model. Final positional parameters are given in the supplementary material.

(55) *International Tables for X-ray Crystallography*; Hahn, T., Ed.; Kynock Press: Birmingham, England, 1974; Vol. IV, pp 99, 149.

Acknowledgment. Funding was provided by the Petroleum Research Fund, administered by the American Chemical Society, and an NSF Presidential Young Investigator award supported by the Monsanto Co. and the Eastman Kodak Co. Washington University's X-ray Crystallography Facility was funded by the NSF Chemical Instrumentation Program (Grant CHE-8811456). The Washington University High-Resolution NMR Service Facility was funded in part by NIH Biomedical Research-Support Shared-Instrument Grant 1 S10 RR02004 and a gift from the Monsanto Co. We thank Dr. Charles Campana from Siemens Analytical X-Ray Instruments, Inc. for collecting the data for compound **1**.

Supplementary Material Available: Tables listing details of the crystallographic data collection, atomic coordinates, bond distances, bond angles, calculated hydrogen atom parameters, and anisotropic thermal parameters (29 pages); listings of observed and calculated structure factors (117 pages). Ordering information is given on any current masthead page.

Complexes with Pt-H-Ag Bonds

Alberto Albinati,[†] Stanislav Chaloupka,[‡] Francesco Demartin,[†] Thomas F. Koetzle,[§] Heinz Rüegger,[‡] Luigi M. Venanzi,*[,‡] and Martin K. Wolfer[‡]

Contribution from the Istituto di Chimica Farmaceutica, Università di Milano, I-20131 Milano, Italy, Chemistry Department, Brookhaven National Laboratory, Upton, New York 11973, and Laboratorium für Anorganische Chemie, ETH-Zentrum, CH-8092 Zürich, Switzerland.
Received May 26, 1992

Abstract: Silver ions react with 2 equiv of the hydrides *trans*-[PtH(C_6X_5)(PR_3)$_2$] (X = F and Cl, R = Me and Et; X = H, R = Et) to give trinuclear complex cations of the type [(PR_3)$_2$(C_6X_5)Pt(μ-H)Ag(μ-H)Pt(C_6X_5)(PR_3)$_2$]$^+$ which were characterized by multinuclear NMR spectroscopy. A full report of the X-ray crystal structure of [(PEt_3)$_2$(C_6Cl_5)Pt(μ-H)Ag(μ-H)Pt(C_6Cl_5)(PEt_3)$_2$](CF_3SO_3) is also given. The silver ion in this complex is linear with two hydride ligands, the H-Ag-H angle being ca. 152°. Significant Pt···Ag direct interactions are also likely to occur. Crystal data: space group $P\bar{1}$, a = 13.853 (3) Å, b = 14.214 (2) Å, c = 15.611 (3) Å, α = 94.64 (2)°, β = 90.48 (2)°, γ = 110.39 (2)°, Z = 2, V = 2869.7 Å^3, ρ(calcd) = 1.875 g cm^{-3}, R = 0.049. The reaction of $AgCF_3SO_3$ and *trans*-[PtH(C_6Cl_5)(PEt_3)$_2$], in a 1:1 ratio, gave the complex [(PEt_3)$_2$(C_6Cl_5)Pt(μ-H)Ag(H_2O)](CF_3SO_3), which was characterized by multinuclear NMR spectroscopy and by X-ray and neutron diffraction. Also in this complex, the silver ion is linearly coordinated. Here, however, it is bonded to one hydride ligand and to one water molecule. Crystal data (neutron, 24 K): space group $P\bar{1}$, a = 8.581 (2) Å, b = 12.053 (3) Å, c = 15.519 (3) Å, α = 87.86 (2)°, β = 73.55 (2)°, γ = 81.76 (2)°, Z = 2, V = 1523 Å^3, ρ(calcd) = 2.105 g cm^{-3}, $R(F^2)$ = 0.081.

Introduction

The affinity of the silver ion for transition metal hydride complexes is now well documented.[1] A general feature of these compounds is the strength of the L_nMH_x·AgL′ interaction.[2] One of the most remarkable classes of compounds with this type of interaction contains a silver ion bonded to two *trans*-[PtH(R)(PR'_3)$_2$] units,[3] with the structure shown schematically as follows:

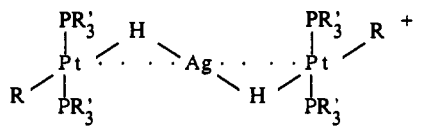

We report here the full characterization of compounds of this type as well as the X-ray and neutron diffraction structures of the related bimetallic compound [(PEt_3)$_2$(C_6Cl_5)Pt(μ-H)Ag(H_2O)](CF_3SO_3).

Results and Discussion

The Trimetallic Pt-H-Ag-H-Pt Complexes. As reported earlier, cationic species of the type [(PR_3)$_2$(C_6X_5)Pt(μ-H)Ag(PR'_3)]$^+$ (**1**) disproportionate in solution as shown in eq 1.

$$2[(PR_3)_2(C_6X_5)Pt(\mu\text{-}H)Ag(PR'_3)]^+ \rightleftharpoons \underset{\mathbf{1}}{} [(PR_3)_2(C_6X_5)Pt(\mu\text{-}H)\underset{\mathbf{2}}{Ag}(\mu\text{-}H)Pt(C_6X_5)(PR_3)_2]^+ + [Ag(PR'_3)_2]^+ \quad (1)$$

[†] Università di Milano.
[‡] ETH-Zentrum.
[§] Brookhaven National Laboratory.

(1) Albinati, A.; Anklin, C.; Janser, P.; Lehner, H.; Matt, D.; Pregosin, P. S.; Venanzi, L. M. *Inorg. Chem.* **1989**, *28*, 1105 and references quoted therein.
(2) Braustein, P.; Gomes Carneiro, T. M.; Matt, D.; Tiripicchio, A.; Tiripicchio Camellini, M. *Angew. Chem., Int. Ed. Engl.* **1986**, *25*, 748.
(3) Albinati, A.; Demartin, F.; Venanzi, L. M.; Wolfer, M. K. *Angew. Chem., Int. Ed. Engl.* **1988**, *27*, 563.

0002-7863/93/1515-169$04.00/0